Simulation of the Fuel Injection System
in Low Speed Diesel Engines

2000 2

ABSTRACT

Diesel invented the compression-ignition engine in 1892. Since that time these engines have continued to develop as our knowledge of engine processes has increased. So, nowadays they play a dominant role in the fields of automobiles, ships and some prime movers. But now worldwide concerns with global climate and environmental protection changed the trend of diesel engine researches to solve the problems how to reduce the pollutant emissions from diesel engines to meet the restrict emission regulations by the IMO(International Maritime Organization).

There are several method that reduce the emission. First of all, the fuel injection system of a diesel engine has taken more important place in understanding of diesel combustion process with combustion chamber, and has taken one of the most important part to prevent environmental pollution by exhaust gas from diesel engine. From this point of view, many investigations have been carried out to solve this problem, such as adopting higher injection pressure and shortening the injection duration by the higher injection rate, etc. Owing to this effort there are considerable improvement to solve pending issues.

But these researches are mainly on the high speed diesel engine or spark ignition engine, therefore it is worth while to study the

low speed diesel engine for ship's use to compare the results which was well known for general trend by the previous researches.

In this study the analysis was carried out by simplifing and modeling the injection phenomena and dividing into three parts comprising of fuel injection pump, high pressure pipe and fuel injection nozzle in the fuel injection system of a low speed diesel engine. A computer simulation model was developed using the Runge-kutta method to solve the equations for each part(fuel injection pump, high pressure pipe and fuel injection nozzle) and the method of characteristics to analyze the unsteady flow in the fuel injection system considering cavitation and variation of fuel density and bulk modulus. Applied was the constant pressure condition at the nodes in the high pressure pipe.

Comparison was commenced between the calculated data and experimental data of pressure and injection quantity at the fuel oil distributor in fuel injection system for the training ship hanara. In the work presented here, the results of a new model which was developed about low speed diesel engine was similar trend to earlist works in the high speed engines. Simulation results about the effect of the high pressure pipe diameter, length, sac volume and efflux coefficient was also analyzed.

NOMENCLATURE

A :   Area (cm2)

B_1 :   First section of Pipe.

B_2 :   Last section of Pipe.

B_3 :   First section of Pipe.

B_4 :   Last section of Pipe.

C :   Efflux coefficient

D :   Diameter of high pressure pipe (cm)

F :   Initial force (Kgf)

K :   Bulk modulus of fuel oil (Kgf/cm2)

k :   Stiffness of spring (Kgf/cm)

M :   Mass (Kgf· s2/cm)

P :   Pressure (Kgf/cm2)

Q :   Volumetric flow rate (cm3/s)

Re :   Reynolds number

U :   Velocity (cm/s)

V :   Volume (cm3)

Y   :   Lift (cm)

a :   Velocity of wave propagation (cm/s)

f :   Darcy-Weisbach friction factor (s-1)

g :   Gravitational constant (cm/s2)

t :   Time (s)

x :   position

ρ :   Fluid density (Kgf· s2/m4)

θ :   Angle (deg.)

λ :   Damping coefficient (Kgf· s/cm2)

Subscript

A,B,C,R,S,P :   Points of x- t Plane

N :   Number of grid in pipe

NS : $N+1$

cyl :   Combustion chamber

e :   Cavitation

sp :   Spill port

h :   Nozzle hole

l :   High pressure pipe

liq :   Liquid

n :   Needle

no :   Area of nozzle valve opening

u :   Plunger

sc : Sac chamber

vap : Vapor

$,j$: Section of j grid at I time for pipe

P,j : Section of j grid at P time for pipe $(P = + \Delta t)$

$,j$: Section of j grid at time for pipe

P,j : Section of j grid at P time for pipe $(P = + \Delta t)$

1

,

.

.

.

.

,   ,

,

.

.1),2)

-           -

3)~6)

.   N O x

,

, Soot

. Soot

,

NOx

.

NOx Soot (Trade off)

. NOx Soot

, ,

- - ,

, , 2 .

,

,

,

.

, , ,

EMS(Engine Monitoring System)

,

, ,

4   -   ,

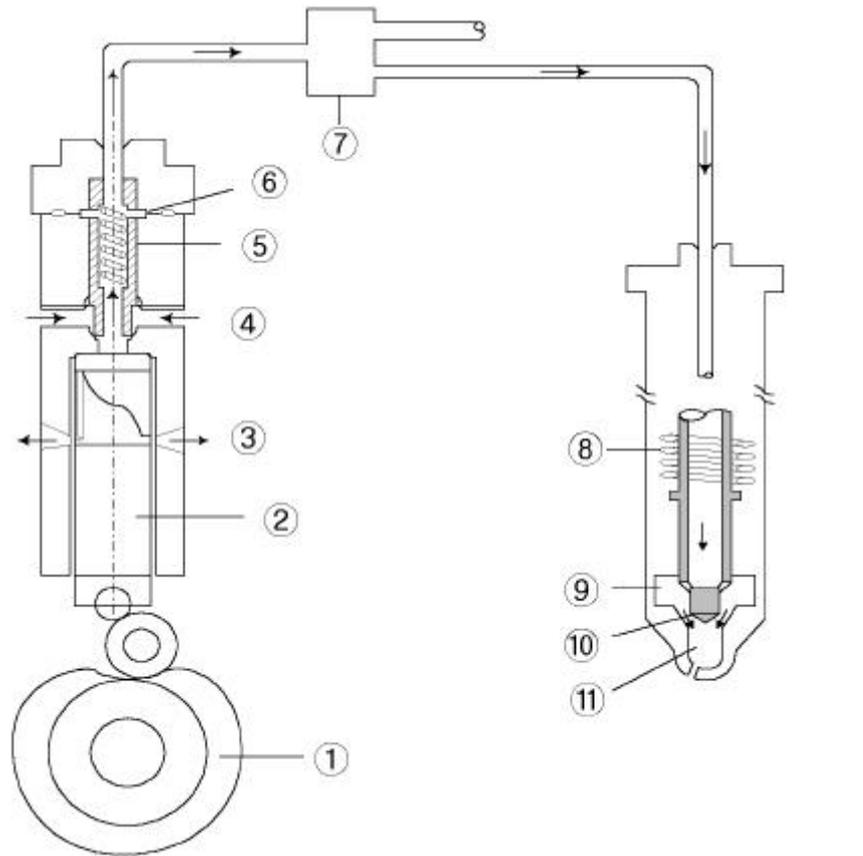   4)   ,

        ,

        5),6)   .

2

2.1

Fig.2-1   ,

                      ,   ,

              (Pipe   )   (Pipe   )   ,

                                                        .

2.2

                                    ,

                              .

(1)   1   ,   .

(2)

              .

(3)   .

(4)   .

(5)

              .   (Spill port)   .

1. Fuel cam	7. Oil distributor
2. Plunger	8. Nozzle spring
3. Spill port	9. Nozzle chamber
4. Intake port	10. Nozzle needle valve
5. Slide valve	11. Sac chamber
6. Delivery chamber	

Fig. 2-1 Schematic diagram of fuel injection system

2.3

2.3.1

$$A_u U_u$$

$$C_{sp} A_{sp} \sqrt{\frac{2}{\rho} [P_u - P_{sp}]}$$

$$A_l U_{1,j} \qquad\qquad\qquad\qquad . \qquad ,$$

$$.$$

$$\frac{dP_u}{dt} = \frac{K_u}{V_u} \left(A_u U_u - C_{sp} A_{sp} \sqrt{\frac{2}{\rho} [P_u - P_{sp}]} - A_l U_{1,j} \right) \qquad (2.1)$$

2.3.2

$$(Sac \; Chamber) \qquad\qquad\qquad\qquad ,$$

$$.$$

$$(1)$$

$$A_l U_{l,j}$$

$$A_n U_n$$

$$C_n A_{no} \sqrt{\frac{2}{\rho} [P_n - P_{sc}]} \qquad\qquad\qquad\qquad .$$

$$\frac{dP_n}{dt} = \frac{K_n}{V_n}\left(A_l U_{l,j} - A_n U_n - C_n A_{no}\sqrt{\frac{2}{\rho}[P_n - P_{sc}]} \right) \qquad (2.2)$$

(2)　　　　　　　　　　　　　　.

M_n

$(A_n - A_{sc})P_n$ 　　　　　　　　　　　　　　$A_{sc}P_{sc}$

F_n,

$\lambda_n U_n$,　　　　　　　　　　　　　　　　$k_n L_n$

.

$$\frac{dU_n}{dt} = \frac{1}{M_n}\left((A_n - A_{sc})P_n + A_{sc}P_{sc} - F_n - k_n L_n - \lambda_n U_n \right) \qquad (2.3)$$

(3)　　　　(Sac Chamber)

.

$$\frac{dP_{sc}}{dt} = \frac{K_{sc}}{V_{sc}}\left(C_n A_{no}\sqrt{\frac{2}{\rho}[P_n - P_{sc}]} - A_h C_h\sqrt{\frac{2}{\rho}[P_{sc} - P_{cyl}]} \right) \qquad (2.4)$$

2.3.3

　　　　　　　　　　1 　　　　　　　　　　　　　　　,

　　　　，　　　　　　　　　　　7)　　　　　　　　　　．

(1)

$$L_1 = \frac{p_x}{\rho} + VV_x + V_t + \frac{fV|V|}{2D} = 0 \qquad\qquad (2.5)$$

(2)

$$L_2 = Vp_x + p_t + \rho a^2 V_x = 0 \qquad\qquad (2.6)$$

f $\dfrac{fV^2}{2D}$

$$\frac{f}{2D} V|V| \qquad\qquad .$$

.

$$L = L_1 + \lambda L_2 = \lambda[p_x(V + \frac{1}{\lambda\rho}) + p_t] + [V_x(V + \lambda\rho a^2) + V_t]$$

$$+ \frac{fV|V|}{2D} = 0 \qquad\qquad (2.7)$$

$$\frac{dx}{dt} = V + \frac{1}{\lambda\rho} = V + \lambda\rho a^2 \qquad\qquad (2.8)$$

(2.8) λ

$$\lambda = \frac{1}{\rho a} \qquad , \qquad (2.9)$$

(2.8) $$\frac{dx}{dt} = V \pm a \qquad . \qquad (2.10)$$

(2.7)   ,

$$\frac{dV}{dt} + \frac{1}{\rho a}\frac{dp}{dt} + \frac{fV|V|}{2D} = 0 \qquad\qquad (2.11)$$

(2.10)   (2.11)   2

.

$$\frac{dV}{dt} + \frac{1}{\rho a} \frac{dp}{dt} + \frac{fV|V|}{2D} = 0 \qquad\qquad (2.12)$$

$$\frac{dx}{dt} = V + a \qquad\qquad (2.13)$$

$$\frac{dV}{dt} - \frac{1}{\rho a} \frac{dp}{dt} + \frac{fV|V|}{2D} = 0 \qquad\qquad (2.14)$$

$$\frac{dx}{dt} = V - a \qquad\qquad (2.15)$$

(2.12) (2.14) x- t plane , (2.12)

(2.13) , (2.14) (2.15) .

(V) (x) (t) x- t

. (V)

(a) .

Fig.2- 2 $\dfrac{\Delta t}{\Delta x}$

.

$$\Delta t(V + a) \le \Delta x$$

Fig.2- 2 P , $t = t_0$

A, B, C A, B B, C R

S $t = t_0 + \Delta t$

(2.12) (2.14) .

,
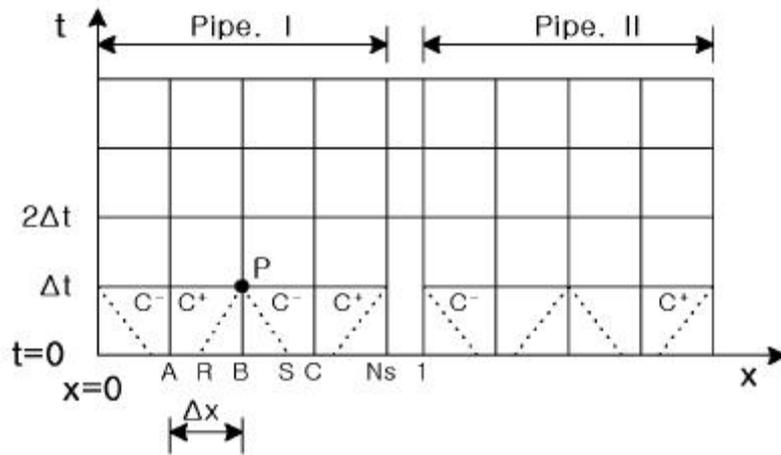
Fig. 2-2 Characteristic lines in the xt **plane.**

Fig.2-3   (Constant pressure)

7)   .

$$H = H_{,NS} = H_{,1}$$

$$Q_{,NS} = Q_{,1} \times 2$$
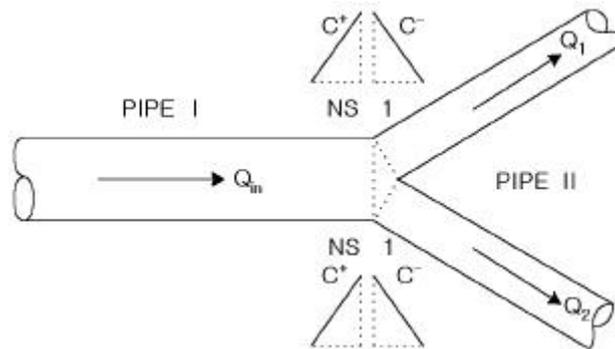
Fig. 2-3 Schematic of a branching connection

2.3.4

(1)　　　　　　　　　　　　（　　　　B 1）

Fig.2- 4　　　　B 1　　　　　　　　　　　　　　　　　　　　　　　　(2.17)

(2.16)　　　　　　　　　$P_{P,1}$　　　　　　　　　　　　　　　　　　　　　　(

)　　　　　　　　　　　　　　(2.18)　　　　　　　　　　　　　　.8)

$$P_{P,1} = a\rho(V_{P,1} - V_S + \frac{1}{a\rho}P_S + \frac{fdt}{2D}V_S|V_S|) \qquad (2.16)$$

$$V_{P,1} = \sqrt{\frac{2(P_u - P_{P,1})}{\rho}} \qquad (2.17)$$

$$V_{P,1} = V_S + \frac{1}{a\rho}(P_{P,1} - P_S) - \frac{fdt}{2D}V_S|V_S| \qquad (2.18)$$

$$V_S = \frac{V_{I,1} - a\dfrac{dt}{dx}(V_{I,1} - V_{I,2})}{1 - \dfrac{dt}{dx}(V_{I,1} - V_{I,2})} \qquad (2.19)$$

$$P_S = P_{I,1} + \frac{dt}{dx}(V_S - a)(P_{I,1} - P_{I,2}) \qquad (2.20)$$

(2)　　　　　　　　　　　（　　　　B 2）

　　　B 2　　　　　　　　　　(2.21), (2.22)

(2.23)　　　　　　　　　　　　　　　　　　　　.

$$P_{P,NS} = a\rho(V_R + \frac{1}{a\rho}P_R - \frac{fdt}{2D}V_R|V_R| - V_{P,NS}) \qquad (2.21)$$

$$V_{P,NS} = \sqrt{\frac{2(P_{P,NS} - P_{,NS})}{\rho}} \qquad (2.22)$$

$$V_{P,NS} = V_R + \frac{1}{a\rho}P_R - \frac{fdt}{2D_I}V_R|V_R| - \frac{1}{a\rho}P_{P,NS} \qquad (2.23)$$

$$V_R = \frac{V_{I,NS} - a\frac{dt}{dx}(V_{I,NS} - V_{I,N})}{1 + \frac{dt}{dx}(V_{I,NS} - V_{I,N})} \qquad (2.24)$$

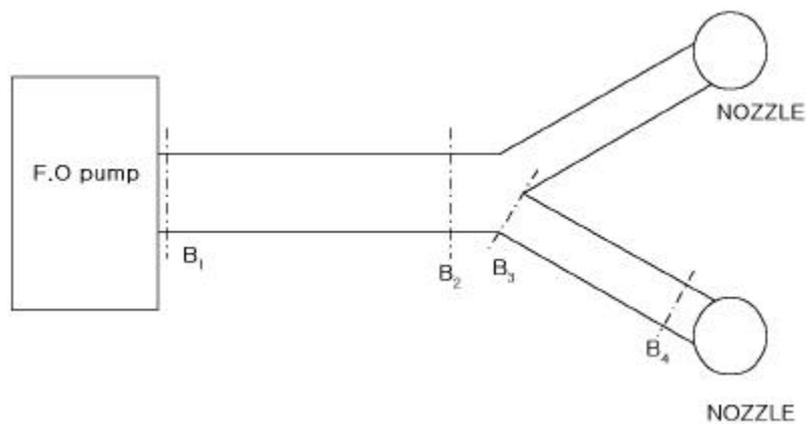$$P_R = P_{I,NS} - \frac{dt}{dx}(V_R + a)(P_{I,NS} - P_{I,N}) \qquad (2.25)$$

（3）   （   B3）

    B3   (Constant Pressure)

            .

$$P_{P,1} = P_{P,NS} \qquad (2.26)$$

$$Q_{P,1} = Q_{P,NS} / 2 \qquad (2.27)$$

（4）   （   B4）

Fig.2-4   B4   (2.29)

(2.28) $P_{P,1}$

（   ）   (2.30)

    8).

$$P_{P,NS} = a\rho(V_R + \frac{1}{a\rho}P_R - \frac{fdt}{2D}V_R|V_R|) \qquad (2.28)$$

$$V_{P,NS} = \sqrt{\frac{2(P_{P,NS} - P_N)}{\rho}} \qquad (2.29)$$

$$V_{P,NS} = V_R + \frac{1}{a\rho}P_R - \frac{fdt}{2D}V_R|V_R| - \frac{1}{a\rho}P_{P,NS} \qquad (2.30)$$

$$V_R = \frac{V_{,NS} - a\dfrac{dt}{dx}(V_{,NS} - V_{,N})}{1 + \dfrac{dt}{dx}(V_{,NS} - V_{,N})} \qquad (2.31)$$

$$P_R = P_{,NS} - \frac{dt}{dx}(V_R + a)(P_{,NS} - P_{,N}) \qquad (2.32)$$

Fig. 2-4 Branching system with fuel pump and nozzle.

2.3.5

(1)   ,

$$\rho = \rho_0(1 + aP - bP^2) \qquad (2.33)$$

$$K = -V\frac{\delta P}{\delta V} = \frac{1 + aP - bP^2}{a - 2bP} \qquad (2.34)$$

ρ_0 , a, b

R.S. Dow   C.E. Fink   9)   .

(2)

f

Darch-Weisbach   .

$$: \quad f = \frac{64}{Re} \tag{2.35}$$

$$: \quad f = 0.00019064 \, Re^{0.64378} \tag{2.36}$$

$$: \quad f = 0.3164 \, Re^{-0.25} \tag{2.37}$$

(3)

(Cavity)

. ρ_e,

K_e

.

$$\rho_e = \rho_i + \frac{\Delta M}{V} \tag{2.38}$$

$$K_e = \frac{K_{vap}}{1 + [(K_{vap} - K_{liq})/K_{liq}]/VL} \tag{2.39}$$

$$VL = \frac{\rho_{liq} - \rho_e}{\rho_{liq} - \rho_{vap}} \tag{2.40}$$

ρ_i Δt , ΔM Δt

. K_e

VL $\rho_{vap} \leq \rho_e \leq \rho_{liq}$

VL . VL

                                                   .

$$VL \geq 1 \qquad VL = 1, \rho_e = \rho_{liq}$$

$$VL < 0 \qquad VL = 0, \rho_e = \rho_{vap}$$

(4)   (Spill port)

     1)
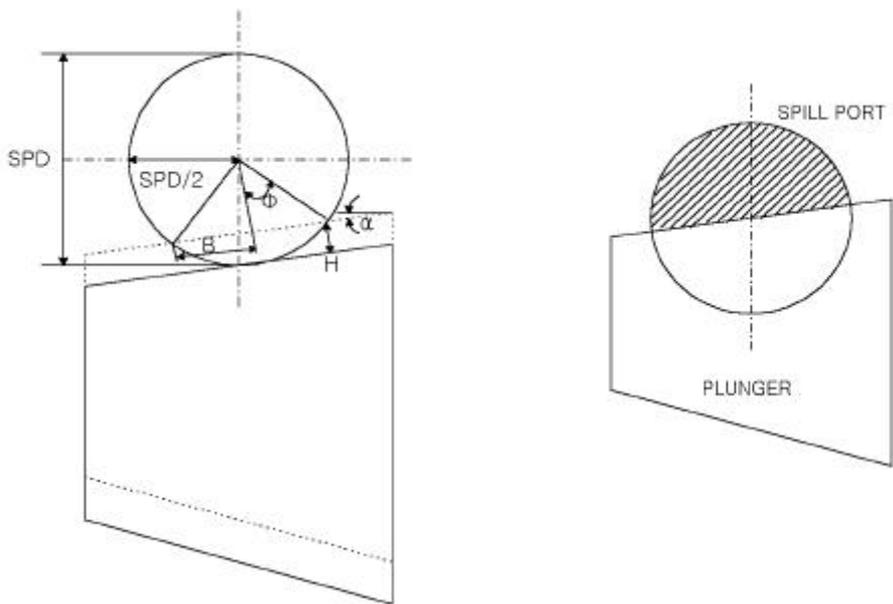
Fig. 2-5   The area of spill port closing

                         H   (2.44)   (XLP)

RPM   (SPC)   ,

    H   10)

$$H = (XLP - SPC) * \cos$$ (2.41)

$$\cos\phi = (\frac{SPD}{2} - H)/(\frac{SPD}{2})$$ (2.42)

$$B = \frac{SPD}{2}\sin\phi$$ (2.43)

$H - SPD/2 \quad 0 \qquad (2.42) \qquad (2.43)$

$$A_{sp} = \frac{\pi - \phi}{4} \cdot SPD^2 + B \frac{SPD}{2}\cos\phi \qquad , \qquad (2.44)$$

$H - SPD/2 \quad 0 \qquad SPD \qquad (2.45) \qquad (2.46)$

$$\cos\phi = (H - \frac{SPD}{2}) / (\frac{SPD}{2})$$ (2.45)

$$B = [H - \frac{SPD}{2}] \tan\phi$$ (2.46)

$$A_{sp} = \frac{\phi}{4} \cdot SPD^2 - B \frac{SPD}{2}\cos\phi \qquad , \qquad (2.47)$$

$H = SPD/2$

$$A_{sp} = \frac{\pi}{8} \cdot SPD^2 \qquad . \qquad (2.48)$$

2)

Fig.2-6 H (XLP),

(ES) (2.49) , H

10)

$$H = [XLP - (ES + SPD + SPC)] \cos\beta$$ (2.49)

$H \quad SPD / 2$

$$A_{sp} = \frac{\phi}{4} \cdot SPD^2 - B \cdot SPD/2 \cdot \cos\phi \qquad , \qquad (2.50)$$

$$H \qquad SPD \ / \ 2$$

$$A_{sp} = \frac{\pi - \phi}{4} \cdot SPD^2 + B \cdot SPD/2 \cdot \cos\phi \qquad , \qquad (2.51)$$

$$H = SPD/2$$

$$A_{sp} = \frac{\pi}{8} \cdot SPD^2 \qquad . \qquad (2.52)$$
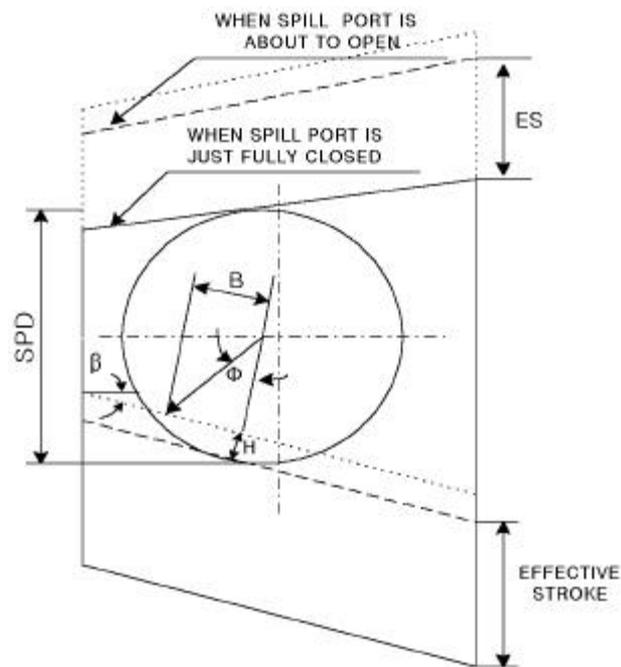
Fig. 2-6 The area of spill port opening

(after the effective stroke)

- 17 -

(5) Nozzle

,

.11)
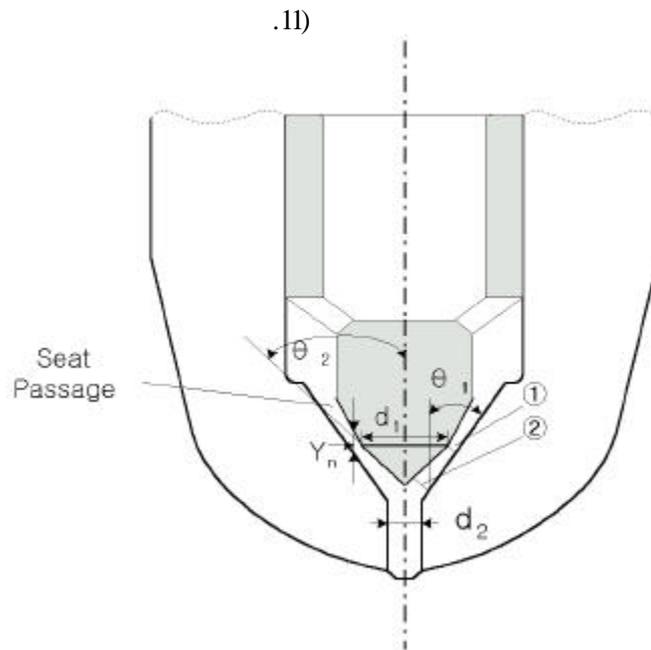
Fig. 2- 7 The flow area through nozzle

$$A_1 = \pi (d_1 + 0.5\, Y_n \sin(2\theta_1)\, Y_n \cos\theta_1) \qquad\qquad (2.53)$$

$$A_2 = \pi [d_2 + \frac{d_1 - d_2}{2} \cos^2(\theta_2) - 0.5(Y_n + \frac{d_1 - d_2}{2} \tan\theta_1)\cdot$$

$$\sin(2\theta_2)]\cdot[Y_n - \frac{d_1 - d_2}{2}(\tan\theta_1 - c\tan\theta_2)]\,\sin\theta_2 \qquad (2.54)$$

(6)

　　　　　　　　　　　，

　　　　　　　　　　　　　　　　　　　　　　　　　　　　　　　　　．

　　　　　　　　　　　　　　　　　　　　　　　　　　，

　　　　　　　　　　．

　　　　　　　　0.6　　0.7　　　　　　　　　　　　　　　　12),13)

　　14)　　　　　　　　，　　　　　　　　　　　0.7,

　　0.6　　　　　　　　　　，

　　0.4　　　　　　　　．

　　　　　　　　　　　　　　8 Kgf/cm 2,　　　　　　　30

Kgf/cm 2　　　　．

2.4

4　　　-　　　　　　　　　　　　　,

2　　　　　　　　　　　　　　　　　.

Fig.2-8　　　.

(1)

,　　　　　,　　　　　　,

.

(2)　　　　　　　　　　　　　　　,

.

(3)　　　　(Pipe　)

.　　　　　　　　　　(Pipe　)

(4)　　　　　　　　　　　　4　　　-

,　　,　　　　　　.

(5)　　　　　　　　$t = t + \Delta t$　　　　　　　.
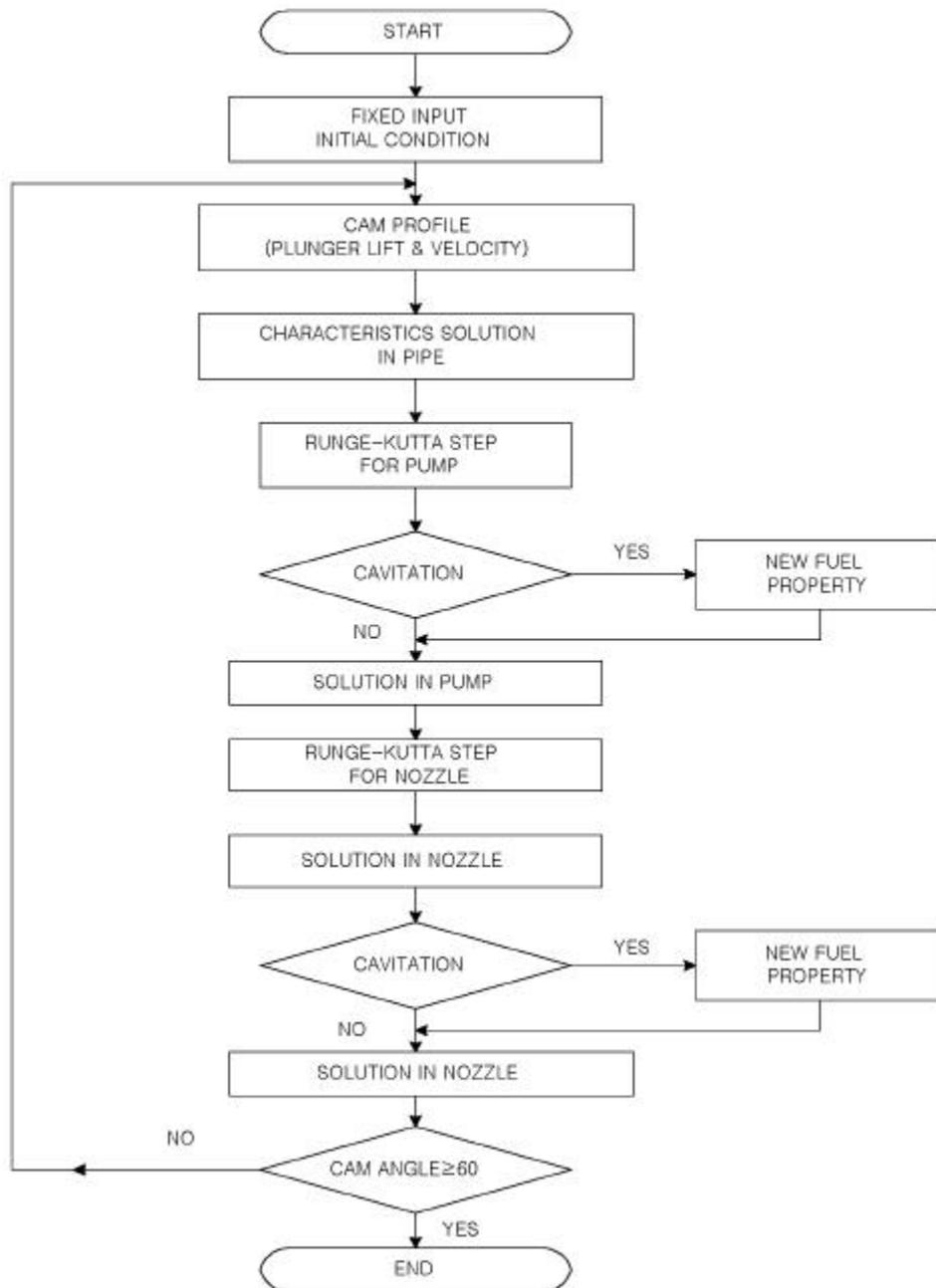
Fig. 2-8 Flow chart

3

3.1

Data   M.A.N.- B&W 6L

35MC   .

Table 2-1 Specification of experimental apparatus

Equipments		Items	Dimension
Fuel pump		Plunger diameter	28.5 mm
		Plunger maximum lift	39.12 mm
		Spill port diameter	2.5 mm
High pressure pipe	Pipe.	Length	716 mm
		Diameter	6.0 mm
	Pipe.	Length	892 mm
		Diameter	4.0 mm
Fuel injection valve		Diameter of needle large end	12.4 mm
		Diameter of needle small end	6.5 mm
		Needle maximum lift	1.6 mm
		Stiffness of spring	24.1 Kgf/mm
		Opening pressure of needle valve	300 Kgf/cm2
		Sac volume	123 mm3
Fuel supply pressure : 8 Kgf/cm2			

3.2　　　　　　　　V IT

3.2.1
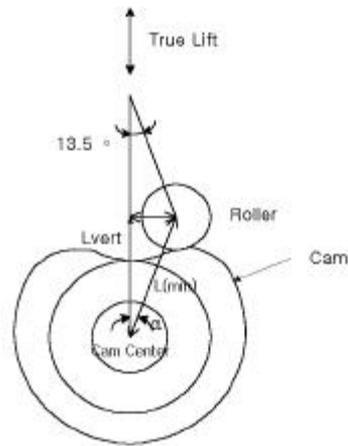
Fig . 3- 1 Fuel cam profile

Fig.3- 1

L   Lvert   ,

(T rue lift)   Fig.3- 2   .
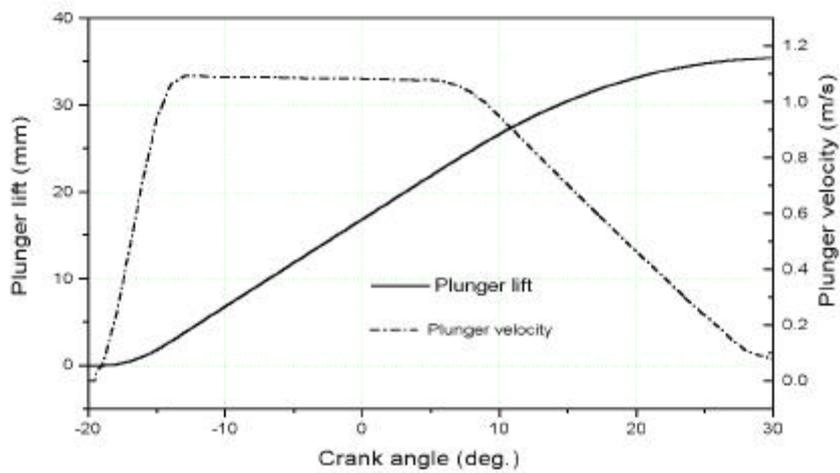
Fig . 3- 2   Plunger lift & velocity

3.2.2 VIT

Fig.3-3   (a)   (Straight edge type)

, (b)   VIT

. Fig.3-4

VIT

(Pmax)   VIT

,

.

VIT

,   4500 PS

(Derating)   85%

.

(a)   (b)
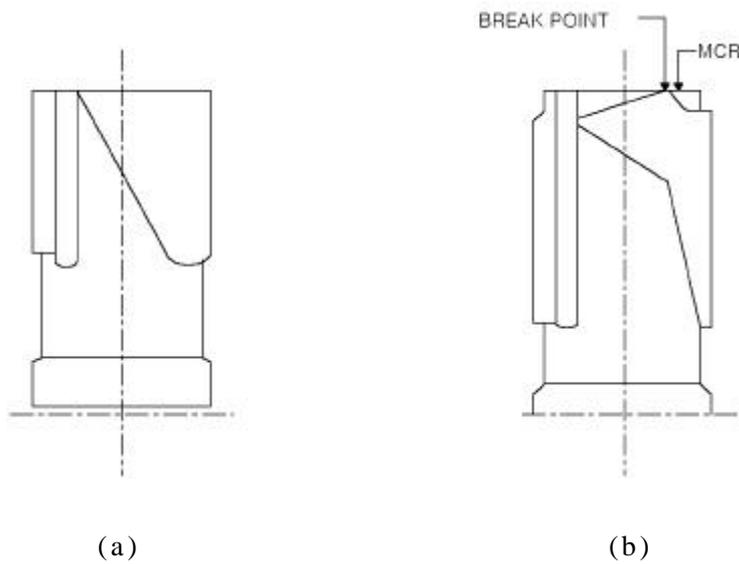
Fig. 3-3 Straight edge Plunger(a) & VIT Plunger(b)
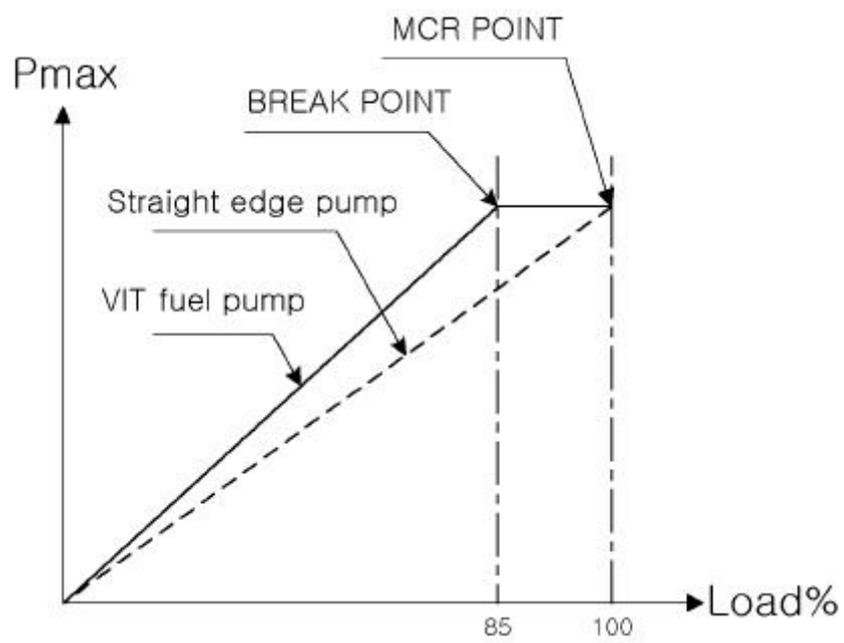
Fig. 3-4   Comparison of Pmax

3.3

3.3.1

EMS(Engine Monitoring System)

,   ,

.   PC

(History)

.

3.3.2 System

(Piezo-tron)

(Junction box)   (Remote control

box)

(Acquistion card)

.

.

, TDC

.
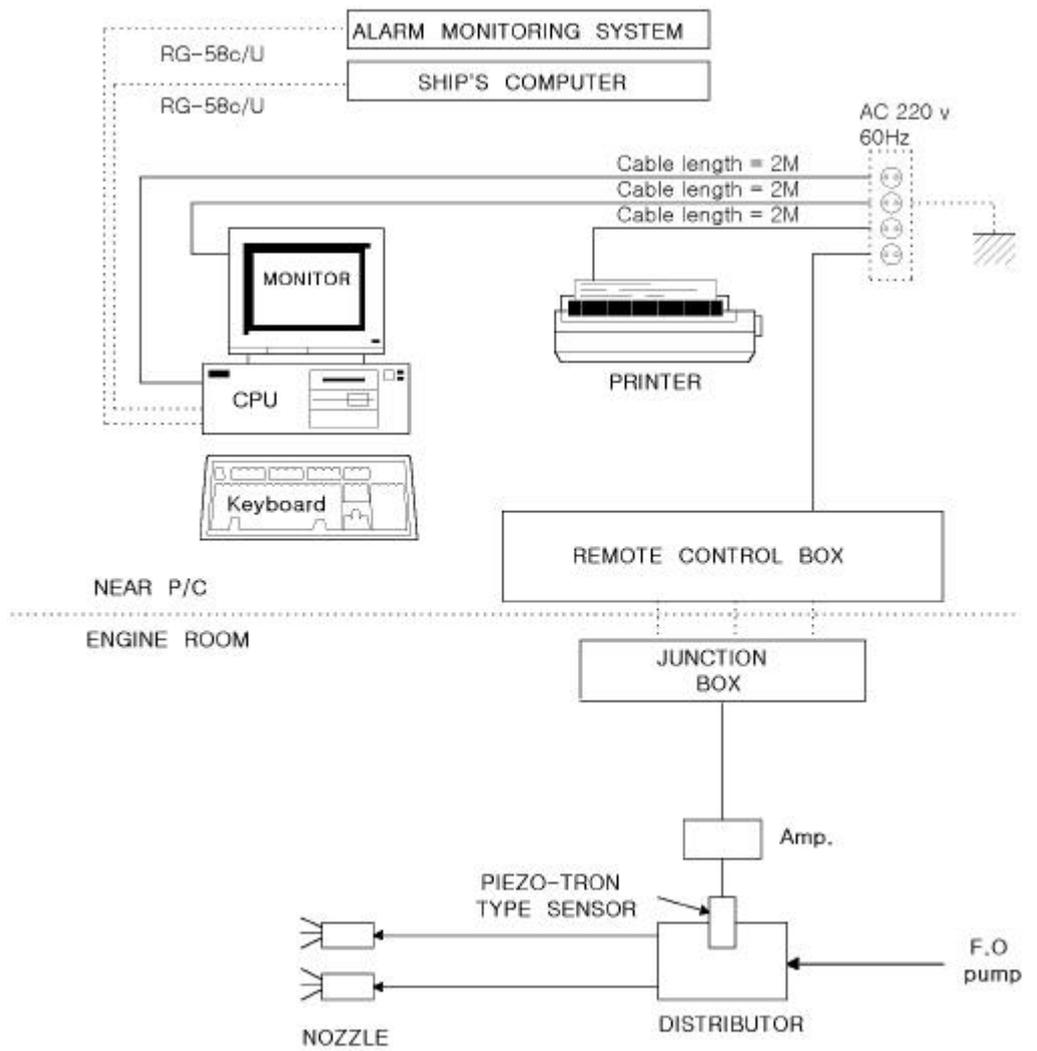
Fig. 3-5 Engine Monitering System(Data acquisition system)

4

EMS

(Distributor)　　　　　　　　　　　　　　，

　　　　　　　　　，　　　，　　　　　　　　　　　．

4.1

Fig.4-1　　　　　　　　　　　　(Distributor)

RPM　　　　　　　　　．

VIT　　　　　　　　　　　　　　　　　，

190　RPM　　　740　Kgf/cm2　　，160　RPM　　　440

Kgf/cm2　　　　　　　　　　　　　　　　　　　．

4.2

Fig.4-2, Fig4-3, Fig4-4　　　RPM

．　RPM　　　　　　　　　3%

　　　　　　　　，

　　．

　　，

．

1   ,

0.01°   .   dt

.

,

(   )

.

Fig.4- 5   RPM

.

(Fuel rack position)

(Break point)   .
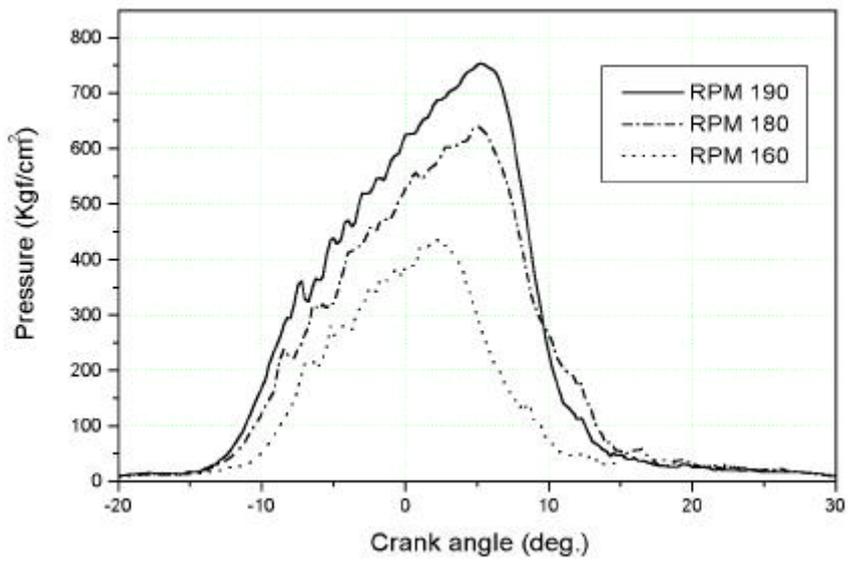
Fig. 4- 1   Experimental results of injection pressure

(at the distributor)

Fig. 4-2 Comparison of simulated and experimental
results (RPM=190)
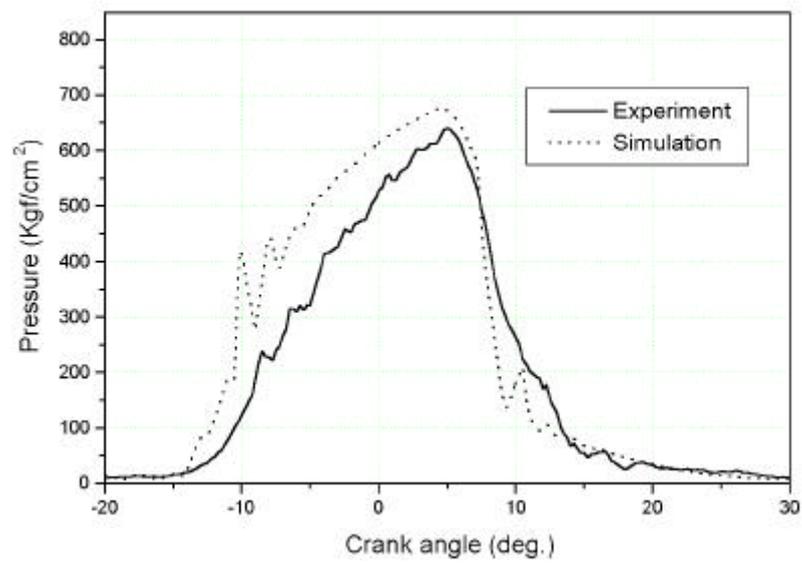
Fig. 4-3 Comparison of simulated and experimental
results (RPM=180)
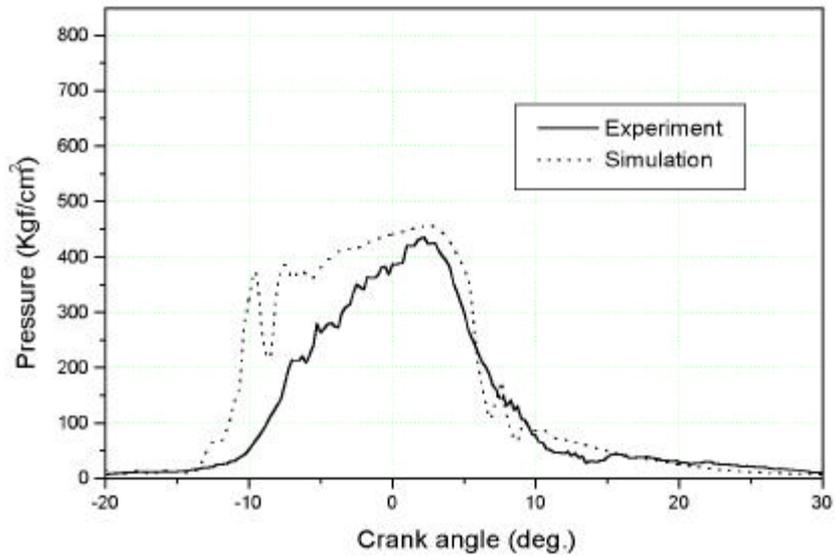
Fig. 4-4 Comparison of simulated and experimental results (RPM=160)
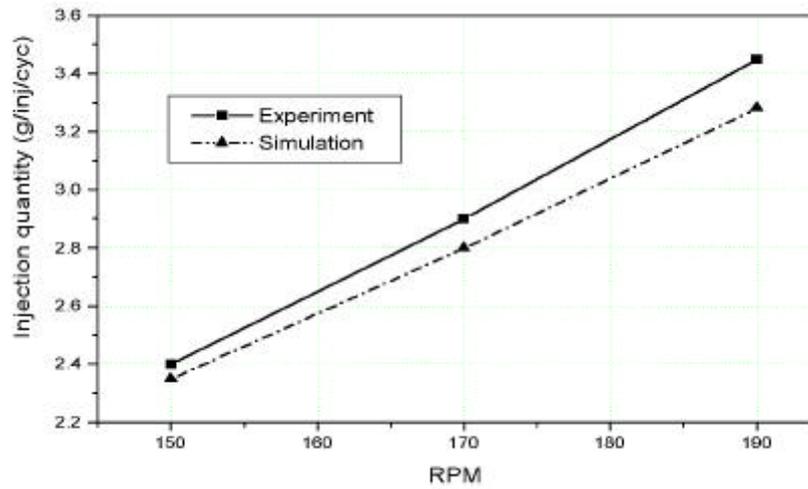
Fig. 4-5 Comparison of simulated and experimental results

4.3

4.3.1

Fig.4- 6   RPM   Fig.4- 7

.

.
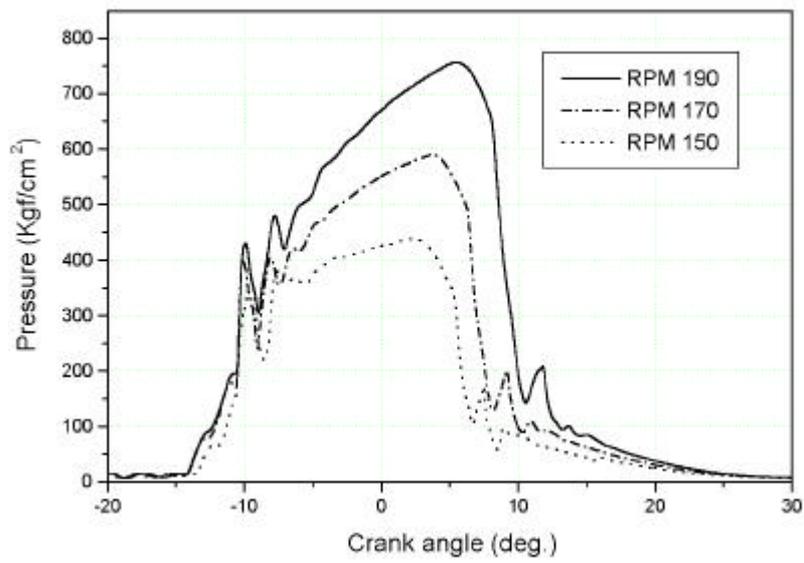
Fig. 4- 6 Injection pressure at various engine speed

(at the distributor)

Fig. 4- 7　Injection rate at various engine speed

4.3.2

Fig.4- 8　　Fig.4- 9

.

,

.
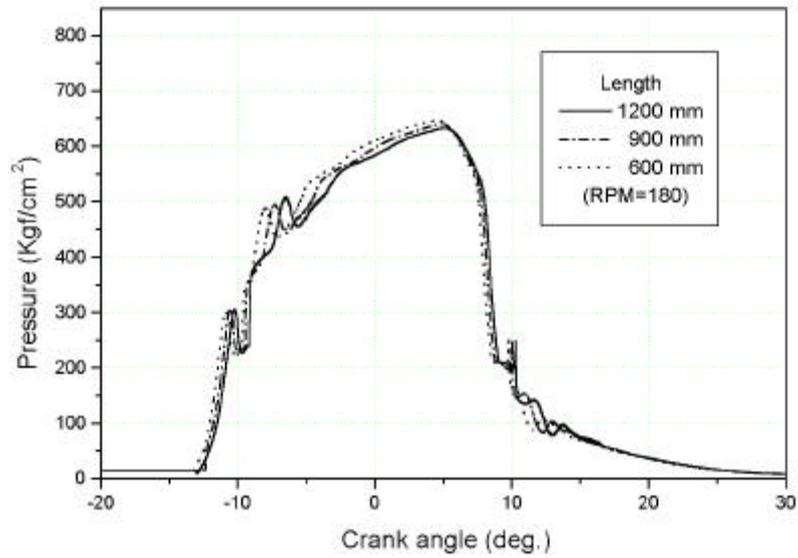
Fig. 4-8 Effect of the high pressure pipe length on
injection pressure(at the nozzle chamber)
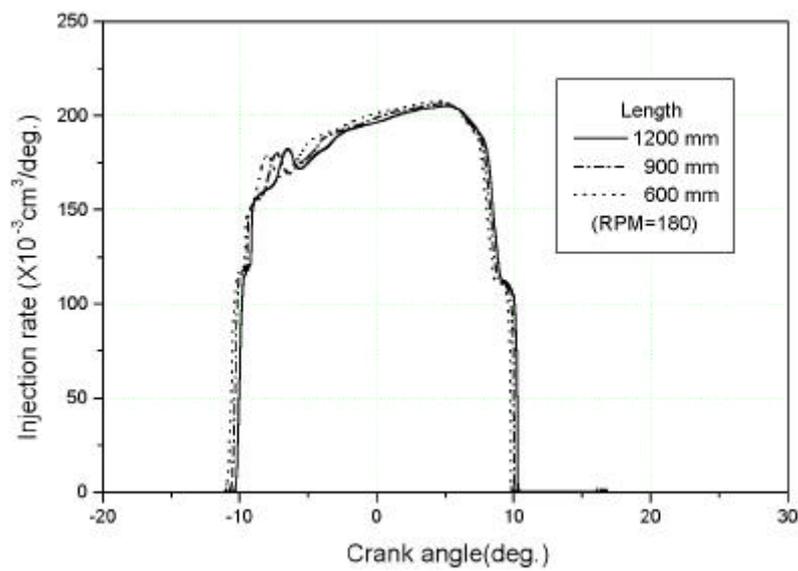
Fig. 4-9 Effect of the high pressure pipe length on
injection rate

Fig.4- 10   Fig.4- 11

.

.
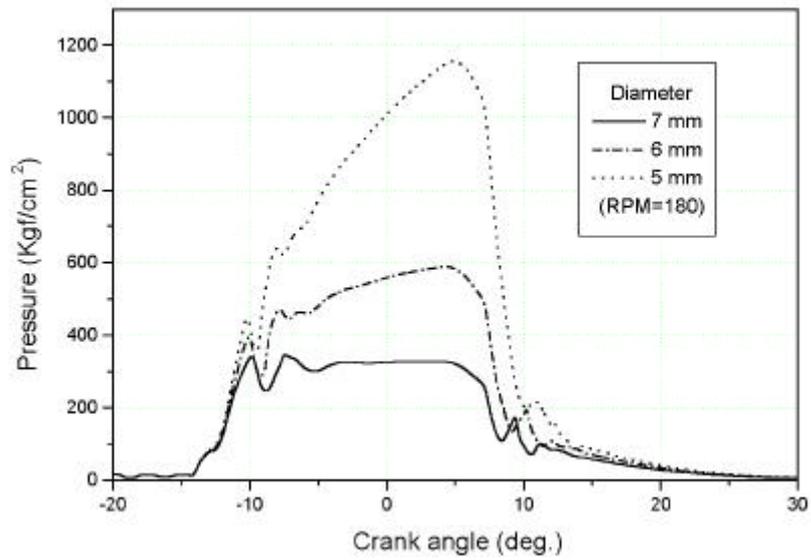
Fig. 4- 10 Effect of the high pressure pipe diameter
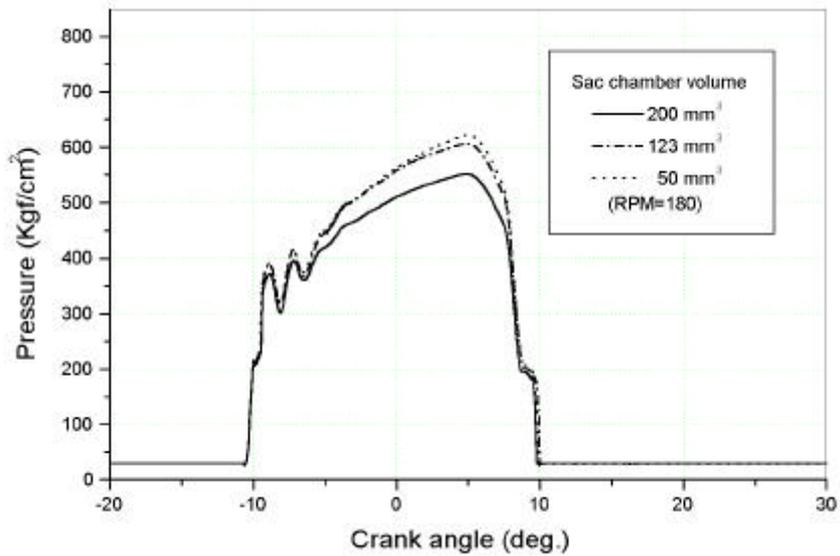on injection pressure (at the distributor)

Fig. 4-11 Effect of the high pressure pipe diameter on injection rate

4.3.3 (Sac volume)

Fig.4-12   Fig.4-13

.

,

.

Fig. 4-12 Effect of the sac volume on injection pressure

(at the sac chamber)
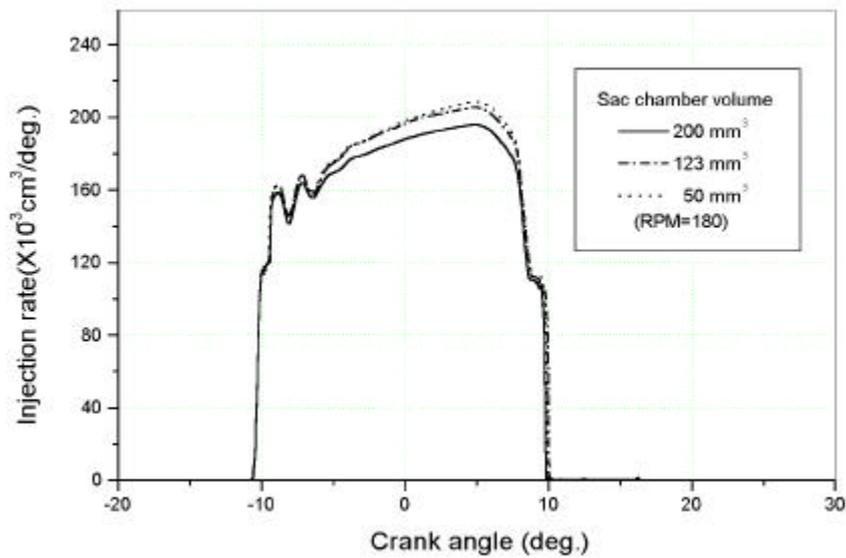
Fig. 4-13 Effect of the sac volume on injection rate

4.3.4

Fig.4-14, Fig.4-15   Fig.4-16

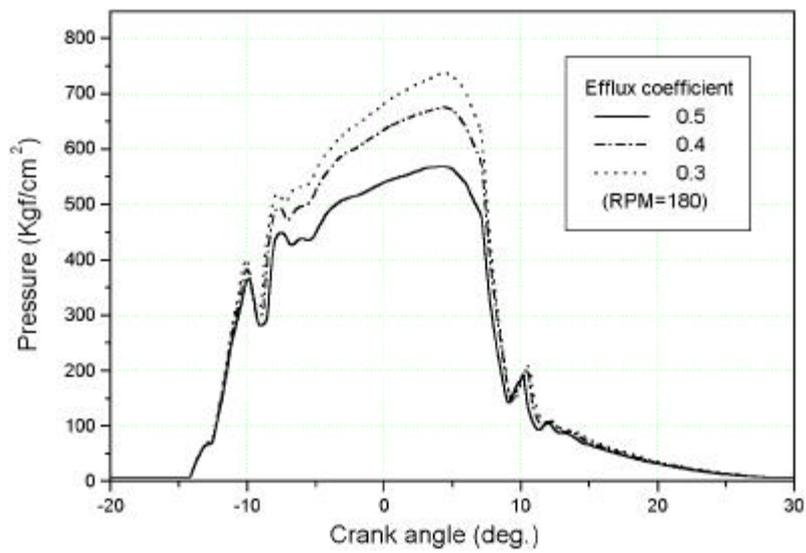,   .

.

.

Fig. 4-14 Effect of the efflux coefficient for pipe
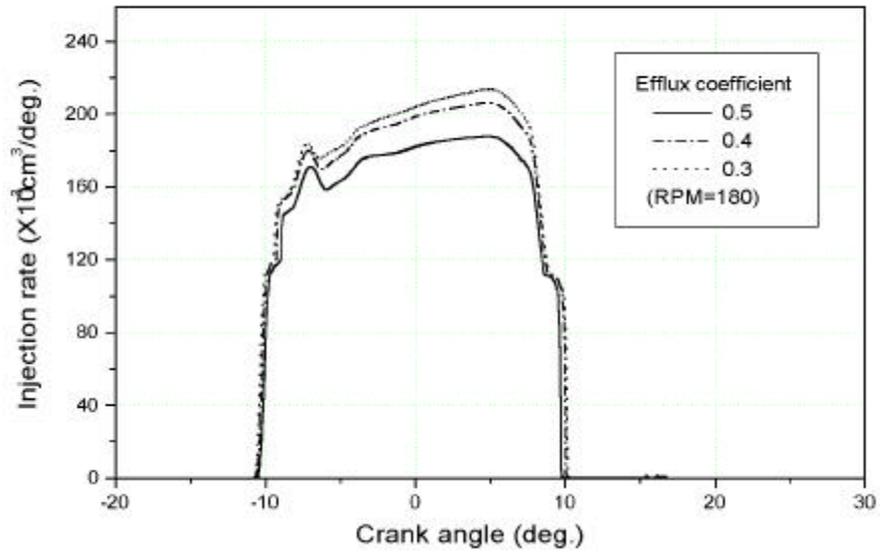
inlet on injection pressure

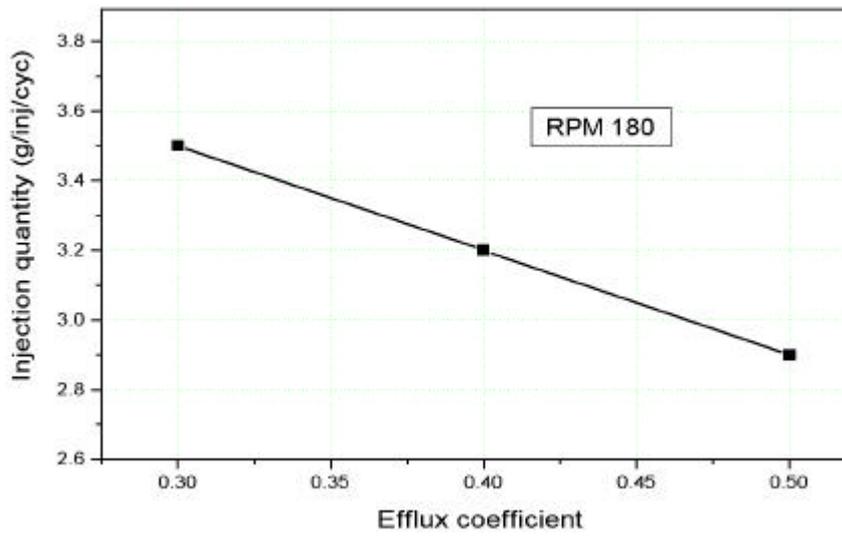Fig. 4-15 Effect of the efflux coefficient for pipe

Fig. 4-16 Effect of the efflux coefficient for pipe

inlet on injection quantity

5

,

.

1)

.

2)

.

3)　　　　　　　(Sac volume)

.

4)

.

(1) T. Kamimoto, "Effect of high Pressure Injection on Soot Formation Processes in a Rapid Compression Machine to Simulate Diesel Flames", SAE No. 871610, 1987.

(2) H. Yokota, "Fast Burning and Reduced Soot Formation via Ultra-high Pressure Diesel Fuel Injection", SAE No. 910025, 1991.

(3) Shin Mastuoka, "A Study of Fuel Injection Systems in Diesel Engine", SAE No. 760551, 1976.

(4) K. Kumar, "A finite Difference Scheme for the Simulation of a Fuel Injection System", SAE No. 831337, 1983.

(5) E. B. Wylie, J. A. Bolt, and M. F. El-Erian, "Diesel Fuel Injection System Simulation and Experimental Correlation", SAE No. 710509, 1971.

(6) G. A. Becchi, "Analytical Simulation of Fuel Injection in Diesel Engines", SAE No. 710568, 1971.

(7) E. Benjamin Wylie, Victor L. Streeter, Lisheng Suo, "Fluid Transients in Systems-Chapter   ,   ."

(8)   , '
         ".   . 1997

(9) R. S. Dow and C. E. Fink, " Computation of Some Physical Properties of Lubricating oils at high Pressure", Journal of Applied Physics, Vol. 2, 1940.

(10) V. Babtiwale and A.Johri "Computer Simulation of Fuel Injection Process in a Diesel Engine", ASME 94-ICE-1

(11)   "Effect of Cam Profile on the Characteristics of P-L-N Diesel Injection System".   . 1992

(12) B. G. Bunting and J. A. Kimberley, "Development of a Square Injection with a Pump-Line-Nozzle System", SAE No. 851581, 1985.

(13) R. Scullen and R. J. Hames, "Computer Simulation of the GM Unit Injector", SAE No. 780161, 1986.

(14) Min Xu, Keiya Nishida and Hiroyuki Hyroyasu, "A Practical and Spray Penetration in Diesel Engine", SAE No. 920624, 1992.